J Appl Electrochem (2008) 38:425–436
DOI 10.1007/s10800-007-9455-5

ORIGINAL PAPER

Chromium electrodeposition from Cr(VI) low concentration solutions

Claudio Fontanesi · Roberto Giovanardi · Maria Cannio · Ercole Soragni

Received: 18 April 2007 / Revised: 14 November 2007 / Accepted: 21 November 2007 / Published online: 5 December 2007

Abstract This work presents a study of a hard chromium plating process using low concentration H_2CrO_4 baths. In particular, the effect of different values of CrO_3/H_2SO_4 ratio on coating properties such as adhesion, hardness, surface roughness, apparent density and microstructure were considered. To increase the solution conductivity, avoiding long deposition times and low throwing power typical of dilute solutions, the behaviour of various inorganic compounds was investigated. Specifically, the compounds suitable for obtaining brighter coatings with lower surface roughness values than those obtained using Fink's solutions were Na_2SO_4 and $Al_2(SO_4)_3 \times 18H_2O$. A bath composition was identified, with a limited use of Cr(VI) in a solution able to produce coatings with a better surface roughness than those of conventional industrial baths.

Keywords Cr(VI) · Coatings · Corrosion · Hard chromium

1 Introduction

The study of chromium electrodeposition is a topic of great practical interest since chromium coatings are used in a variety of industries to confer particular mechanical properties and decorative finishes to metal parts. Functional chromium coatings consist of a thick layer of chromium (from 1.3 to 300 μm) to provide a surface with functional properties such as corrosion resistance, hardness and wear resistance [1–13]. Decorative chromium coatings consist of a thin layer of chromium (0.003–0.5 μm) that lends a shiny, wear- and tarnish-resistant surface when plated over a nickel layer.

The electrodeposition processes used to deposit both hard and decorative chromium coatings are still based on the operative conditions established by Fink's patent in 1926 [14]: (i) deposition bath made up of an aqueous solution containing CrO_3 and H_2SO_4 with a weight ratio 100:1 (normally 250 and 2.5 g dm^{-3}, respectively) (ii) working temperature of about 50 °C (iii) current densities from 0.200 to 0.400 A cm^{-2}. Although electrochemical deposition can be performed at constant current, due to the difficulties in measuring the exact area of complex shaped pieces, voltage control is preferred. Current efficiency seldom reaches 18%, as most of the current supplied to the cell is dissipated through the hydrogen reduction reaction.

The use of CrO_3 compounds is discouraged as they are toxic, carcinogenic and can cause permanent genetic changes; moreover its oxidising nature makes CrO_3 dangerous for the environment [15, 16].

One way to overcome these drawbacks would be to deposit chromium coatings from solutions of trivalent chromium salts, which do not present the same hazards for human health and for the environment. Unfortunately, coatings obtained using Cr(III) solutions are unsatisfactory, as in aqueous solutions the Cr(III) ions form highly stable aqueous complexes. To minimise this problem an appropriate ligand capable of forming a Cr(III) complex with optimum chemical and electrochemical reactivity can be used [4]; however, state of art Cr(III) plating still presents several technical issues, such as low current efficiency and solution instability.

C. Fontanesi
Department of Chemistry, University of Modena and Reggio Emilia, Via Campi 183, Modena 41100, Italy

R. Giovanardi (✉) · M. Cannio · E. Soragni
Department of Material Engineering, University of Modena and Reggio Emilia, Via Vignolese 905, Modena 41100, Italy
e-mail: giovanardi.roberto@unimore.it

One way to restrict the heavy environmental impact of highly concentrated solutions and cut the high costs of processing fluid disposal could be the use of weaker solutions.

This work considers the effect of altering some of the process variables of Fink's patent, especially by evaluating the influence on mechanical properties and the corrosion resistance of hard chromium coatings. The Faradaic efficiency of the whole process was also considered amongst the important evaluation criteria and particular attention was focussed on coatings obtained using dilute Cr(VI) solutions.

The effect of the sulphate anions present in the deposition bath is also investigated. Experimental evidence has shown that a 100:1 ratio between the concentration of chromium trioxide and sulphuric acid is optimal, as expected on the basis of the reduction reaction mechanism stochiometry [2, 3].

In this study, the CrO_3:SO_4^{2-} ratio was varied between 1:40 and 1:200, by modifying either the chromium oxide or sulphate concentration. Table 1 summarises the chemical composition of the electrolytic solutions investigated.

One problem arising from the use of dilute solutions is a decrease in the throwing power due to the decrease in solution conductivity. Throwing power is related to the ionic strength of the plating bath, which regulates the ability of the bath to produce a good and smooth deposit even on objects with complicated surfaces (e.g. holes, notching and knurling) assuring a uniform potential distribution. Throwing power is experimentally determined using a Haring-Blum cell and, amongst the several expressions used to calculate its value, the most frequently employed Field formula is [17]:

$$\text{Throwing power} = \frac{(K - M) \cdot 100}{K + M - 2} \quad (1)$$

where $K = x_1/x_2$ and $M = W_2/W_1$, x_1 and x_2 are the distances of the first and second cathode, respectively from a single anode and W_2 and W_1 are the weight of metal plated on the two cathodes. This equation is designed to give throwing powers of between +100 (very good) and −100 (very poor).

Finally, the addition of an ionic compound, which does not give chemical or electrochemical parasitic reactions, to maintain the ionic strength of the dilute solution at the same value of the traditional concentrated solution, was investigated. The ionic compound must satisfy certain requirements: (a) high solubility in aqueous solutions (b) high chemical stability in the presence of a strong oxidising agent at very low pH (c) electrochemical stability in the potential region needed for massive chromium deposition; the additive must not undergo reduction reactions, which could worsen the coating quality and further reduce current efficiency.

Sulphate containing compounds able to increase the ionic strength even at low concentration without significantly altering the $[CrO_3]/[SO_4^{2-}]$ ratio, such as $Al_2(SO_4)_3 \times 18$ H_2O and Na_2SO_4, were selected. Since the addition of sulphate anions influences the reaction mechanism, a detailed study of the effects of the additives at several concentrations was considered. Bath compositions are reported in Table 2.

Table 1 Chemical composition of the different electrolytic solutions

Solution	$[CrO_3]$ (g dm^{-3})	$[SO_4^{2-}]$ (g dm^{-3})	Concentration ratio
1	100	2.50	40/1
2	250	6.25	40/1
3	200	2.50	80/1
4	250	3.12	80/1
5	100	1.00	100/1
6(Fink)	250	2.50	100/1
7	500	5.00	100/1
8	250	1.25	200/1
9	500	2.50	200/1

2 Experimental

Figure 1 shows the cell used for the electrochemical chromium deposition tests. This cell was specifically designed to simulate the industrial electrodeposition of chromium: the working electrode was introduced from the bottom of the cell and its particular shape allowed the hydrogen evolved at the cathode to flow out of the cell easily in conditions of high overvoltage and high current density. A platinum ring counter electrode was positioned

Table 2 Composition of the electrolytic solutions studied to evaluate the effect of concentration of SO_4^{2-} ion; all of them were prepared with the same concentration of CrO_3, 100 g dm^{-3} (dilute solutions)

Solution	$[CrO_3]$ (g dm^{-3})	$[SO_4^{2-}]$ (g dm^{-3})	Additive	[Additive] (g dm^{-3})
0HA	100	0.5	H_2SO_4	0.510
1HA	100	1.0	H_2SO_4	1.021
2HA	100	2.0	H_2SO_4	2.042
5HA	100	5.0	H_2SO_4	5.104
0Al	100	0.5	$Al_2(SO_4)_3 \times 18H_2O$	1.156
1Al	100	1.0	$Al_2(SO_4)_3 \times 18H_2O$	2.312
2Al	100	2.0	$Al_2(SO_4)_3 \times 18H_2O$	4.625
5Al	100	5.0	$Al_2(SO_4)_3 \times 18H_2O$	11.562
0Na	100	0.5	Na_2SO_4	0.739
1Na	100	1.0	Na_2SO_4	1.479
2Na	100	2.0	Na_2SO_4	2.957
5Na	100	5.0	Na_2SO_4	7.393

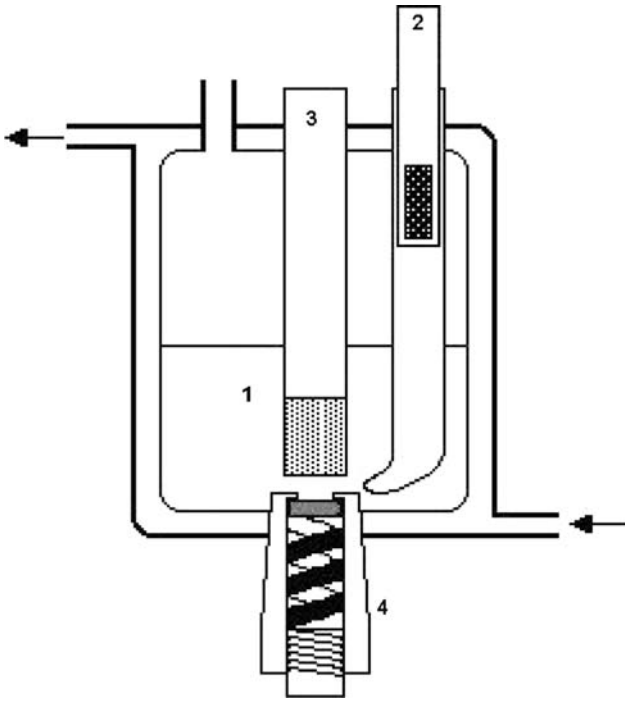

Fig. 1 Working cell used for the electrochemical process (1) solution, (2) reference electrode, (3) counter electrode, (4) working electrode (sample)

above the working electrode, as near as possible to the substrate, in order to guarantee the best current distribution and reduce electrolyte resistance. The reference electrode was a saturated calomel electrode (SCE); in the present work all potential values are referred to SCE.

The working electrode was a carbon steel disc with the following composition: $\%^{m}/_{m}$ 0.28 C, 0.33 Si, 0.60 Mn, 0.023 S. The exposed surface area was 1.0 cm^2, previously polished with silicon carbide emery paper up to grade 800, to remove superficial oxides and to control surface roughness. After the mechanical pre-treatment, the specimens were washed and degreased in acetone. The current efficiency was evaluated by weighing the specimens before and after the chromium deposition.

Solutions were prepared using CrO_3 (Aldrich Chem. Co.), H_2SO_4, $Al_2(SO_4)_3 \times 18H_2O$, Na_2SO_4 (Carlo Erba R.P.E.) in distilled water ('reagent grade' Millipore MilliQ).

Electrochemical deposition was carried out in a four-step cycle under potentiostatic control: (i) cathodic polarisation from the rest potential (about 0.850 V) to −1.800 V (scan rate 10 mV s^{-1}); (ii) constant potential for 10 s; (iii) return to −1.500 V with the same scan rate; (iv) constant potential for the rest of the test length (1 or 5 h). An EG&G Mod. 270 programmable Galvanostat-Potentiostat was used.

All measurements and tests were performed at constant temperature (50 ± 1) °C.

2.1 Coating characterisation

Chromium coatings obtained using the electrochemical procedure described above were characterised by recording and analysing data concerning:

(i) the morphology of the surfaces and cross sections by means of SEM photomicrographs performed using a Philips XL40 microscope; the section was obtained by cutting the samples with a REMET Micromet and mechanically polished using a Buehler Minimet 1000 (Buehler emery paper and alumina 0.05 μm);
(ii) coating thickness measured by a thickness gauge (SONATEST) and compared with SEM observations;
(iii) apparent density, calculated as ratio of the deposit weight (mg) and the coating volume (surface area × thickness, cm^3), the latter quantity is useful to evaluate the presence of pores, microcracks and gaseous inclusions;
(iv) surface roughness determined using a DIAVITE DH5 profilometer (traversing length 4 mm, cut off 0.8 mm);
(v) corrosion resistance using Tafel plots from −300 to +300 mV with respect to the rest potential (scan rate 0.2 mV s^{-1}) in a H_2SO_4 0.1 M aqueous solution; the extent of the corrosion attack was evaluated by observation of the samples using an optical metallographic microscope (REICHERT MeF2);
(vi) scratch tests were carried out with 'PLST progressive load procedure' [18], using the following parameters: Rockwell indenter of diameter 400 μm, scratch length 1 mm, lateral displacement speed 0.5 mm min^{-1}, load change from 0.1 to 30 N (loading rate 15 N min^{-1});
(vii) micro-hardness, measured using a WOLPERT 401 MVD Micro-hardness Tester, with a 0.980 N load and 15 s indentation time; the indentation was performed on the section of the coatings, obtained by cutting the samples using a REMET Micromet and mechanically polished using a Buehler Minimet 1000 (Buehler emery paper and alumina 0.05 μm).

3 Results and discussion

3.1 Microstructural analysis

Figures 2 and 3 show SEM images of the top surface and of the cross section of the nine coatings obtained using bath compositions reported in Table 1 after 1-h deposition time, respectively. On a qualitative level, the chromium deposit morphology, typical of a traditional solution (Fig. 2, solution 6) is also observed in coatings obtained using

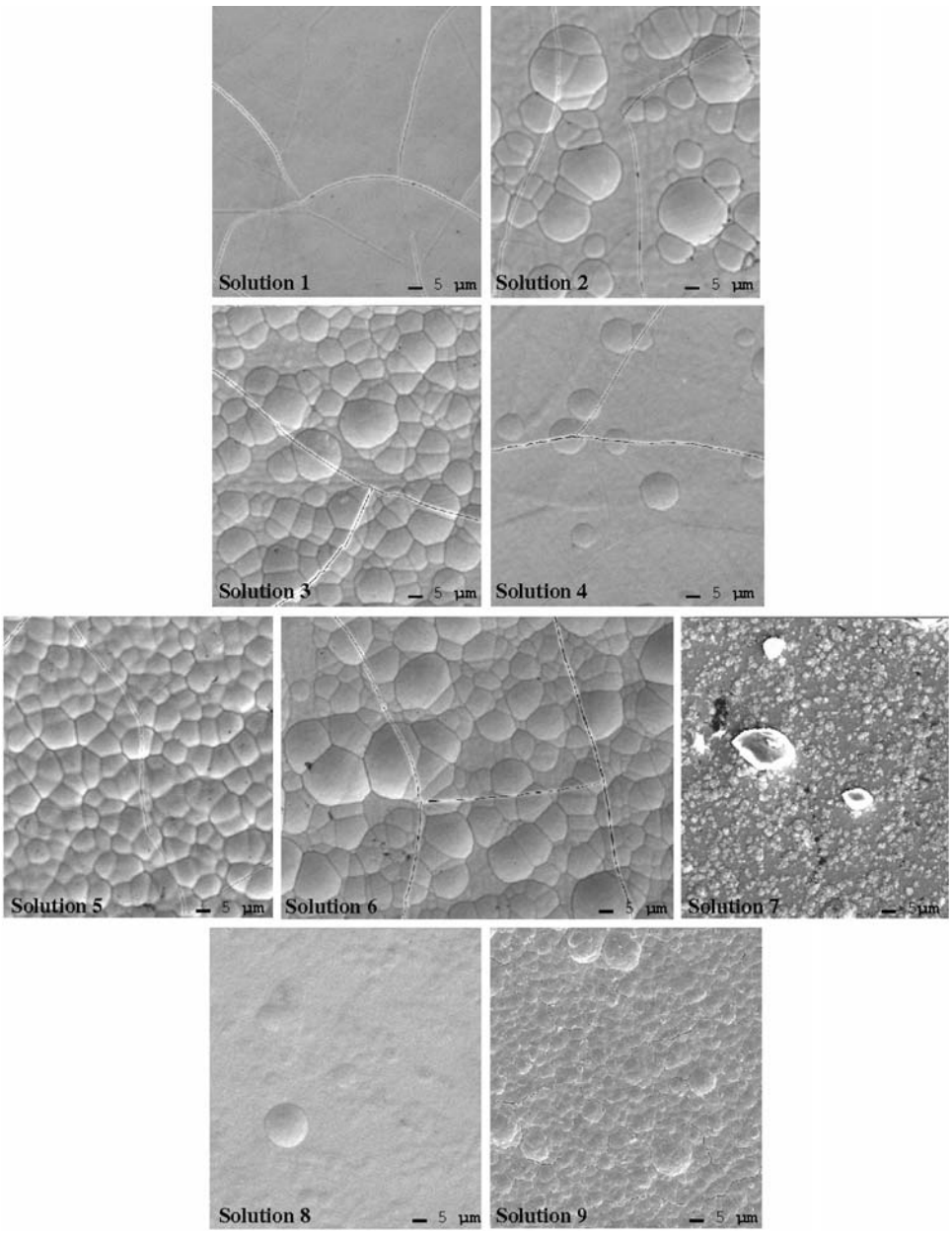

Fig. 2 SEM micrographs (surface) of the coatings obtained by electrodeposition using solutions 1–9 (see Table 1 for composition)

solutions of different chemical composition. Baths 2, 3, and 5 (Table 1) provide optimal results both considering the surface morphology (almost free of large cracks) and the microstructure of the cross section (high thickness deposits).

The presence of microcracks in chromium coatings is a spontaneous phenomenon caused by internal stress relief, decreasing the deposit brittleness. However, in order to ensure protection against corrosion, these cracks must not be so deep as to allow the aggressive medium to reach the substrate, as is shown in the deposit obtained from solution 9 (Fig. 3).

Cross section analysis reveals that the deposit from solution 5 follows the metal support profile very closely; this behaviour, of course, suggests a remarkable adhesion of the coating to the substrate. For this reason, amongst the solutions that showed good behaviour (numbers 2, 3, and 5), solution 5 can be considered the most promising one, at least from a morphological point of view. Bath 5 has the same $[CrO_3]/[H_2SO_4]$ conventional ratio (100:1), but lower chromium trioxide content (100 g dm^{-3} instead of 250 g dm^{-3}).

Finally, the deposit obtained from solution 8 is thin and has very few cracks (Fig. 3 shows a single macro defect, probably due to a pre-existing substrate imperfection). This bath composition can be chosen for those applications where the properties of corrosion resistance must be prioritised.

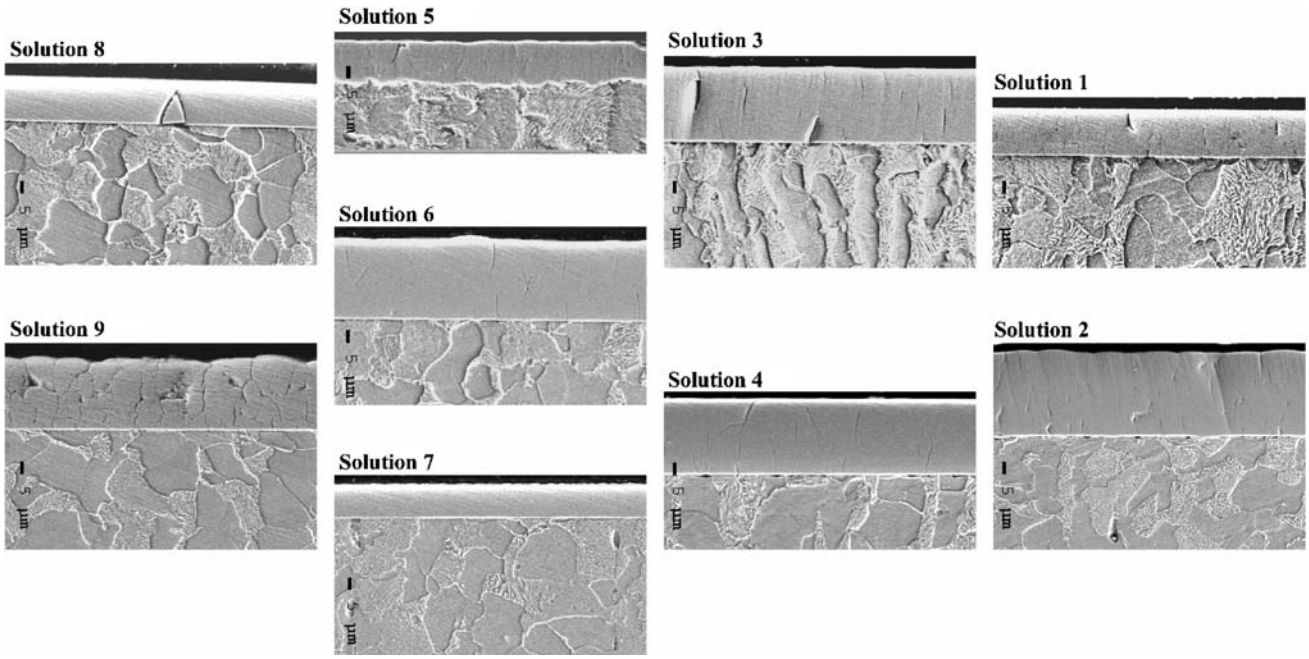

Fig. 3 SEM micrographs (cross section) of the coatings obtained by electrodeposition using solutions 1–9 (see Table 1 for composition)

3.2 Faradaic efficiency

Faraday's first law allows the determination of the current efficiency [19] according the equation:

$$6\,n_{\mathrm{Cr}} = n_{\mathrm{e}} = \frac{i_{\mathrm{m}}\,t}{F} \tag{2}$$

where n_{Cr} and n_{e} are numbers of moles of deposited chromium and the moles of electrons supplied, respectively, i_{m} is the mean current flowing, t is the electrolysis time, F is Faraday's constant, and 6 refers to the number of electrons involved in the electrochemical reaction. The chromium moles can be expressed as a mass giving the following relationship:

$$\Delta W = \frac{i_{\mathrm{m}}\,t\,\mathrm{AW_{Cr}}}{6\,F} \tag{3}$$

ΔW is the mass of electrodeposited chromium and $\mathrm{AW_{Cr}}$ is the atomic weight of the chromium (51.996 g $\mathrm{mol^{-1}}$). Equation 3 allows calculation of the chromium mass deposited in ideal conditions (current efficiency, $\eta\% = 100\%$). For 1-h depositions, the time was set as 3,960 s: the time that elapsed during the initial potentiodynamic step (360 s) was added to the 1 h time of electrodeposition at constant potential. The current was also averaged over this time interval.

The ratio between the experimentally determined weight uptake after electrodeposition, ΔW_{meas}, and theoretical, ΔW, gives the current efficiency, according to the equation:

$$\eta\% = \frac{\Delta W_{\mathrm{meas}}}{\Delta W} \times 100 \tag{4}$$

The i_{m}, ΔW_{meas} and $\eta\%$ data obtained for the nine solutions examined are shown in a bar graph in Fig. 4a, b. The analysis of these data allows us to draw a number of conclusions:

- the efficiency threshold of 18–20% was never exceeded. This limit concerns the hydrogen evolution reaction that dissipates most of the current supplied to the cell, as for conventional baths.
- all the solutions with a high CrO_3 content (500 g $\mathrm{dm^{-3}}$) yield low current efficiency; together with the strong hazards coming from the use of chromium trioxide. This result allows us to exclude the possibility of working with alternative baths with high chromium contents.
- the solutions with low CrO_3 content (specially the solution 5) give a good Faradaic efficiency, such as that obtained with the traditional bath (solution 6). It must be pointed out that i_{m} is proportional to the theoretical ΔW through the constant $K = t\mathrm{AW_{Cr}}/6F$, so, under the same ΔW_{meas}, the efficiency $\eta\%$ will be greater the smaller the current i_{m} (Eqs. 2 and 3).

This also means that coatings with low weight increase (ΔW_{meas}) and low deposit thickness can show high efficiency at low current; one good example is provided by the

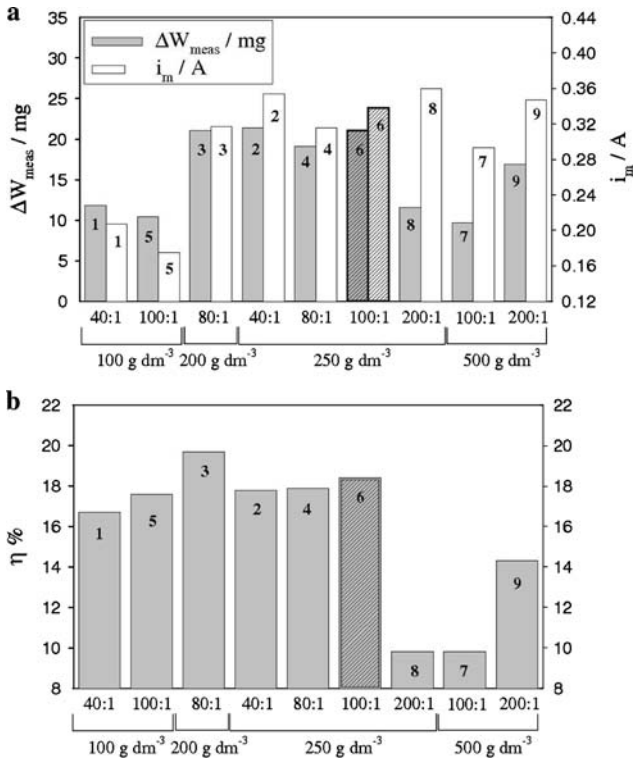

Fig. 4 Weight uptake of electrodeposited chromium ΔW_{meas} and average current i_m (**a**), Faradaic yield, $\eta\%$ (**b**) for the different samples deposited by the solutions described in Table 1

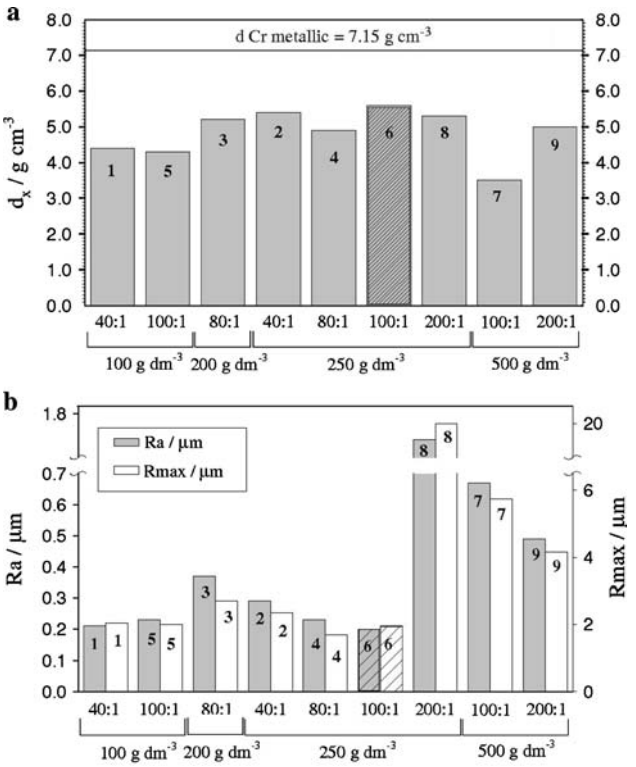

Fig. 5 Apparent density (**a**) and surface roughness (maximum and average) (**b**) of the different coatings

deposit from solution 5, which at the same impressed potential shows an i_m of about half that of the standard bath. Obviously, when the former is used, double time is needed to obtain coatings of the same thickness, although Faradaic yield is almost the same.

3.3 Apparent density

The weight increase (ΔW_{meas}) and the measured thickness (h_{meas}) data allow calculation of the coating apparent density (d_x). This parameter gives useful information about the deposit porosity: the lower d_x the more the coating is porous or cracked.

Since all the specimens have a 1.0 cm^2 exposed electrode surface, d_x (g cm^{-3}) is given by the ratio ΔW_{meas} (g)/h_{meas} (cm). The bar graph of Fig. 5a shows the calculated d_x values as compared with the value of the metallic chromium density (7.15 g cm^{-3}, horizontal line). All the values of d_x are smaller than 6 g cm^{-3}, this means that hydrogen occlusions and microcracks are present in all the coatings. This phenomenon is enhanced in the deposit from solution 7, which shows a d_x value of 3.5 g cm^{-3} (about half the density of metallic chromium). If on the one hand the presence of microcracks and little occlusions decreases internal stresses (hence the brittleness), on the other hand, it should compromise the deposit hardness and protection capacity. Coatings with poor mechanical properties can be expected from solution 7.

3.4 Surface roughness

In Fig. 5b, the values of mean (R_a) and maximum (R_{max}) roughness of the examined specimens are compared. Some clear differences must be pointed out: the concentrated CrO_3 solutions give very rough deposit surfaces of poor technological interest; the dilute solutions (specially solutions 1 and 5) give coatings with very low surface roughness. In some cases, the roughness is lower than that achieved by conventional deposits (solution 6).

Table 3 summarises these results; to evaluate the role played by the chemical composition, a symbol "+" was attributed to the parameters that seem better than those obtained using the "conventional" bath (++ the best); conversely, the symbol "−" means that the parameters considered are worse than those obtained using a conventional bath (−− the worst). When no symbols were reported, the parameter is similar to that obtained using Fink's patent.

The solutions with chromium trioxide concentration below or equal to 250 g dm^{-3} yield the best results, supporting the idea that dilute baths can be efficiently used in industrial applications.

Table 3 Summary of results for the characterisation of the coatings; the effect of the bath composition is taken into consideration: the symbol "+" means that the considered parameter is comparable to or better than that of a conventional bath, and "−" is used when the parameter examined is poorer than that of a conventional bath

Solution	$[CrO_3]$ (g dm^{-3})	$[H_2SO_4]$ (g dm^{-3})	Concentration ratio	Surface morphology	Section Morphology	$\eta\%$	d_x	R_a
1	100	2.50	40/1			+	+	++
2	250	6.25	40/1	+	+	+	+	+
3	200	2.50	80/1	+	+	++	+	−
4	250	3.12	80/1		+	+	+	+
5	100	1.00	100/1	++	++	+	+	++
6 (Fink)	250	2.50	100/1	xx	xx	xx	xx	xx
7	500	5.00	100/1	−	−	−−	−	−
8	250	1.25	200/1		−	−−	+	−−
9	500	2.50	200/1	−−	−−	−	+	−

3.5 Scratch test

To check hardness and adherence of the coating, scratch tests were carried out with variable loads (0.1–30 N); deposits from highly concentrated solutions (numbers 7 and 9) were neglected, because previous examinations had proven that they are unsatisfactory. Moreover, their high surface roughness would make it hard to obtain sensitive scratch test results. All tested deposits showed very similar behaviour: the picture of the scratch test trace for coating number 2 is shown in Fig. 6. Results can be summarised as follow: (i) chromium coating detachment never occurs, even in the heaviest load conditions; (ii) the spread and the widening of pre-existent cracks on the surface are the first sign of failure, particularly along the sides of the indenter trace; the first critical load is recorded in relation to this phenomenon, as shown in Fig. 6 by marker 1; (iii) new cracks, perpendicular to the scratch direction, appear as the applied load increases; the second critical load is recorded in relation to this phenomenon (Fig. 6, marker 2).

The values of the critical loads obtained are shown in Table 4. The differences amongst the various samples are almost negligible: the first critical load is always between 4 and 8 N, the second above 8 N. The most important

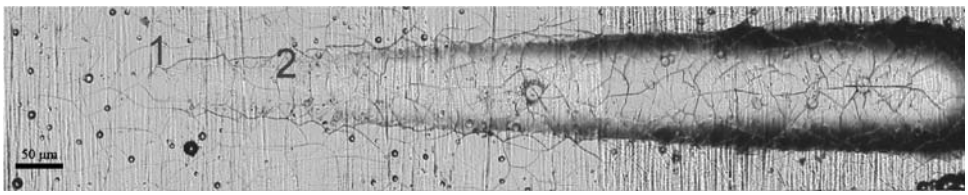

Fig. 6 Image acquired with metallographic microscope on coating obtained with solution 2, after scratch test (progressive load from 0.1 N to 30 N); markers '1' and '2' identify, respectively, the formation of lateral (first critical load) and transversal (second critical load) cracks on the coating, respectively

Table 4 Scratch tests results

Solution	$[CrO_3]$ (g dm^{-3})	$[H_2SO_4]$ (g dm^{-3})	Ratio	Critical loads (N)	
				Lateral cracks	Transverse cracks
1	100	2.50	40/1	6.80	6.80
2	250	6.25	40/1	5.18	8.89
3	200	2.50	80/1	7.97	11.9
4	250	3.12	80/1	5.66	13.58
5	100	1.0	100/1	8.72	17.3
6 (Fink)	250	2.50	100/1	4.82	8.96
8	250	1.25	200/1	8.53	8.53

consideration is that all the values are comparable with (and even better than) those recorded for coatings using the conventional solution (6).

It is well known that the different loads are usually attributed to the presence of pre-existing cracks at the point where the test is performed. None of the coatings investigated detached from the base metal; however the cracks were seen to spread and new cracks developed. This feature is of utmost importance for hard chromium applications.

3.6 Micro-hardness

The values of micro-hardness (HV) for the coatings obtained from different bath compositions are shown in Table 5; as for scratch test analysis, the deposits prepared from high-concentration solutions (7 and 9) were rejected, as previous results had shown them to be unsatisfactory.

The values reported in Table 5 were obtained as the mean of at least three indentations performed in different positions on the coating section.

Table 5 Micro-hardness results

Solution	$[CrO_3]$ (g dm^{-3})	$[H_2SO_4]$ (g dm^{-3})	Ratio	HV
1	100	2.50	40/1	879.2
2	250	6.25	40/1	780.8
3	200	2.50	80/1	1007.0
4	250	3.12	80/1	1027.0
5	100	1.0	100/1	1041.7
6 (Fink)	250	2.50	100/1	938.2
8	250	1.25	200/1	936.1

Table 6 Characterisation of the coatings obtained with 1-h depositions and 5-h depositions

Solution	1-h Depositions			5-h Depositions		
	η%	R_a (μm)	i_m (mA)	η%	R_a (μm)	i_m (mA)
0Na	17.2	0.07	148	15.9	0.20	170
1Na	18.7	0.11	177	17.4	0.24	165
2Na	17.3	0.09	175	16.3	0.14	163
5Na	10.9	0.07	173	–	–	–
0Al	20.1	0.13	162	16.4	0.26	183
1Al	17.5	0.09	119	19.5	0.22	180
2Al	22.1	0.12	169	17.4	0.18	168
5Al	12.7	0.04	169	–	–	–
0HA	18.5	0.21	184	16.6	0.29	172
1HA	19.8	0.12	188	18.1	0.24	179
2HA	18.7	0.17	185	17.8	0.27	175
5HA	12.7	0.05	179	–	–	–

Hard chromium coatings obtained using Fink's bath usually have micro-hardness values greater than 900 Vickers. Therefore, all the coatings analysed have acceptable values of HV, except for those obtained from solutions 1 and 2 (the two solutions with the lowest $[Cr_2O_3]$:$[H_2SO_4]$ ratio).

A high H_2SO_4 concentration probably emphasises the hydrogen occlusion phenomenon in the coatings, leading to

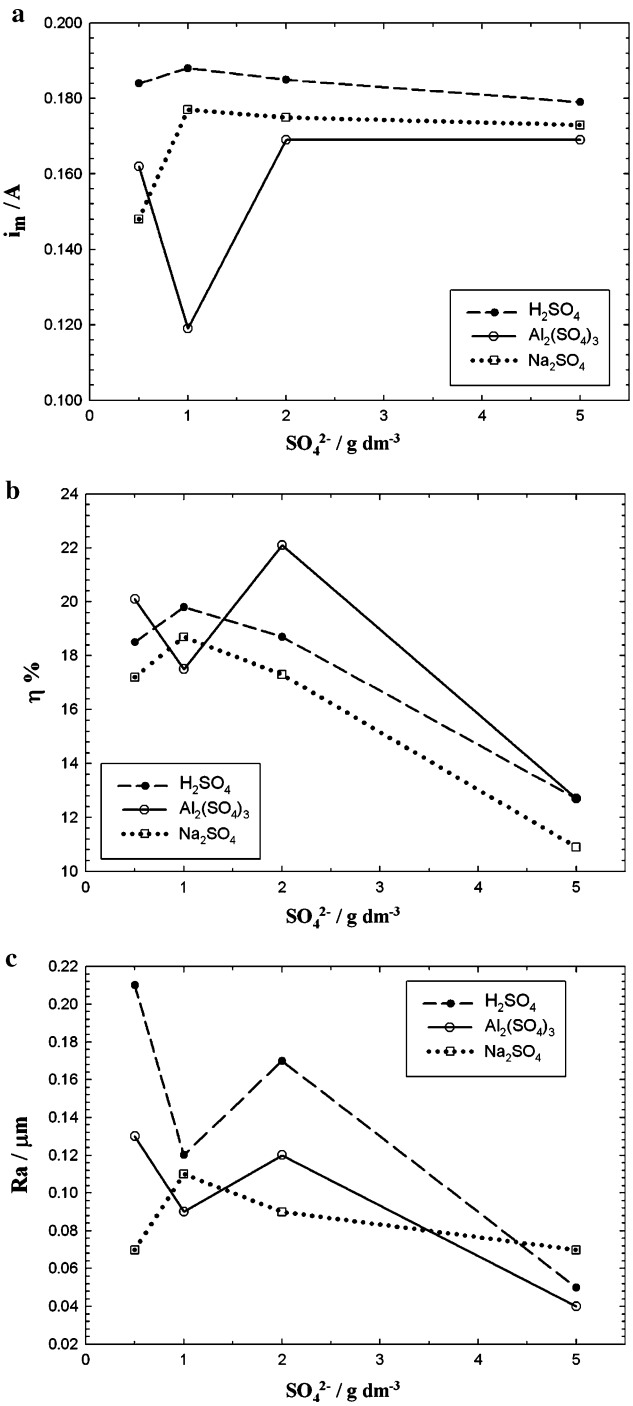

Fig. 7 Influence of additives on average current (**a**), Faradaic yield (**b**) and average roughness (**c**)

deposits with low hardness and poorer mechanical resistance.

All other micro-hardness values are comparable with (and often better than) those of coatings obtained using a traditional solution (6). In particular, solution 5 shows the higher value.

All the tests performed show that solution 5 (CrO_3 100 g dm^{-3}) gives good quality deposits, and, for this reason, could constitute an effective alternative to industrial concentration baths. However, from an industrial point of view, the use of solution 5 implies two problems: (1) under voltage control, double output times are needed to use this bath; (2) the lower electrical conductivity can influence the throwing power of the bath and hence coating evenness. We therefore sought a suitable additive to increase the solution ionic strength without affecting the deposition process.

3.7 Use of additives

The compositions of several solutions used to investigate the influence of various additives are listed in Table 2. The coatings obtained over 1 h were characterised taking into account the morphology, the Faradaic efficiency and roughness, as in the previous cases. Results are shown in Table 6, together with the i_m values.

The following conclusions can be drawn:

(1) the i_m value does not depend strictly on the kind and concentration of the additive (Fig. 7a); this result is disappointing, as the goal was to increase the mean current;
(2) current efficiency drops sharply when the sulphate ion concentration exceeds 2 g dm^{-3} (Fig. 7b), and, as a rule, it does not undergo great changes according to the used additive;
(3) the average roughness is much lower using Na_2SO_4 and $Al_2(SO_4)_3$ rather than sulphuric acid (Fig. 7c); this unexpected result is certainly important, since a smoother surface improves the wear resistance in those applications involving metal surface coupling;
(4) the deposit morphology is influenced by sulphate ion contents (Figs. 8, 9, and 10): in particular, the baths with a high SO_4^{2-} content give more homogeneous and smoother surfaces characterised by the presence of thinner microcracks. This fact confirms the extremely low roughness values observed with solutions containing 5 g dm^{-3} of sulphate ions.

The addition of sodium sulphate and aluminium sulphate did not achieve the aim of increasing the mean current but it did make it possible to obtain better quality deposits in terms of surface roughness. To confirm these

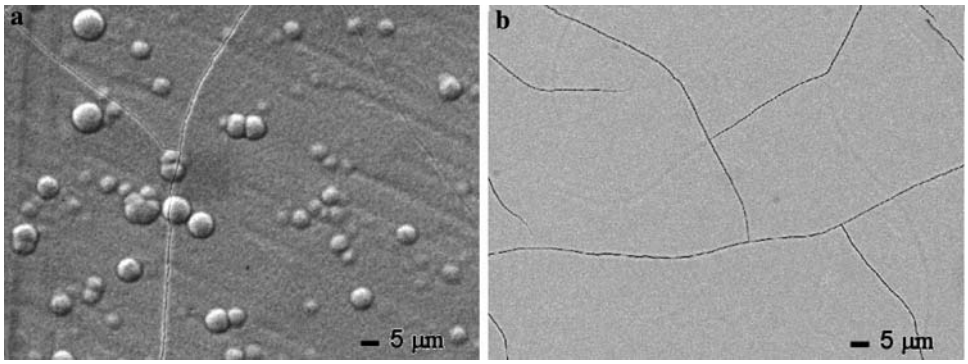

Fig. 8 SEM micrographs: effect of Na_2SO_4 on surface morphology; (**a**) Na_2SO_4 0.5 g L^{-1}; (**b**) Na_2SO_4 5.0 g L^{-1}

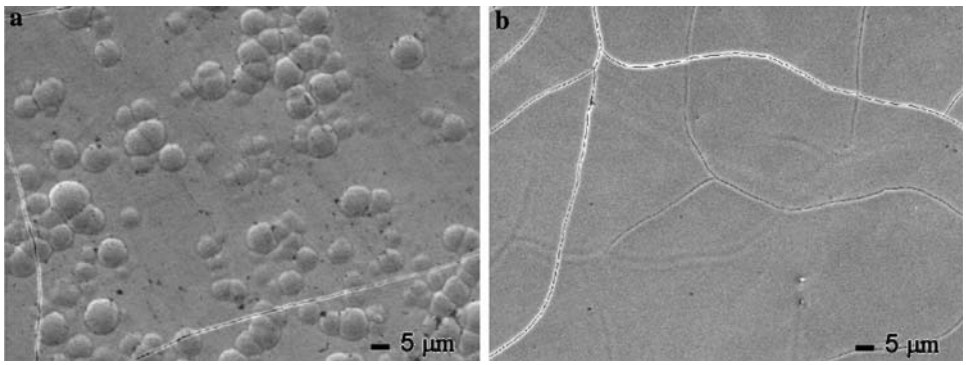

Fig. 9 SEM micrographs: effect of $Al_2(SO_4)_3 \times 18H_2O$ on surface morphology; (**a**) $Al_2(SO_4)_3 \times 18H_2O$ 0.5 g L^{-1}; (**b**) $Al_2(SO_4)_3 \times 18H_2O$ 5.0 g L^{-1}

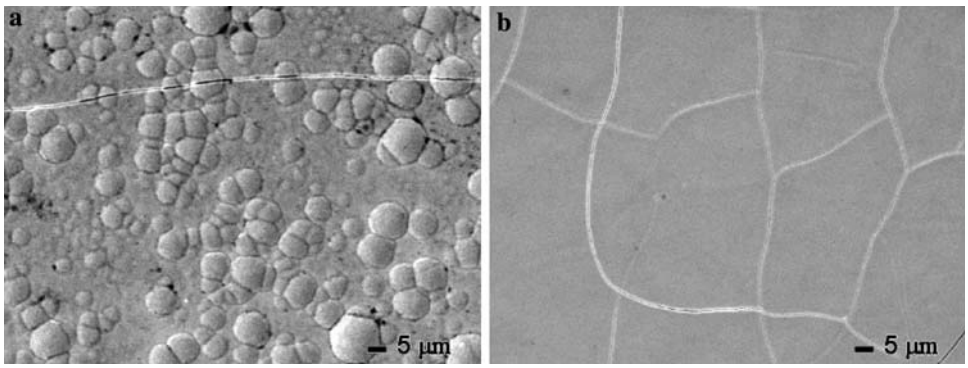

Fig. 10 SEM micrographs: effect of H_2SO_4 on surface morphology; (**a**) H_2SO_4 0.5 g L^{-1}; (**b**) H_2SO_4 5.0 g L^{-1}

results, 5-h depositions were performed on rough steel surfaces (polished with emery paper 800 mesh). The aim was to prove the possibility of producing low roughness deposits even on substrates with surfaces such as those used in industrial plants. Solutions with sulphate ion concentrations of 5 g dm^{-3} were not taken into account due to their low current efficiency. Results are given in Table 6 and show an average roughness decrease when Na_2SO_4 or $Al_2(SO_4)_3$ is used, rather than H_2SO_4; this decrease is more evident when the SO_4^{2-} concentration is 2 g dm^{-3}. Current efficiency does not vary significantly.

No additive has been identified as being able to solve the problems involved in the use of solution 5 as an industrial bath. This solution yields good coatings and could represent a valid alternative to the concentrated solutions currently used: longer deposition times could be accepted on account of the bath's lower environmental impact. Although more time is needed to obtain a good deposit, the current employed is the same of that used with Fink's solution and a better coating is achieved, especially concerning roughness. This suggests the use of these coatings for special high quality finishes such as applications where friction properties are paramount. In any case, the search for new additives led to the discovery of certain solutions (1Na and 1Al, Table 2) that yield coatings with better properties. Most notably, surface roughness is greatly improved.

Another important property of chromium coatings is corrosion resistance. In order to study the corrosion resistance of deposits obtained from dilute solutions, electrochemical corrosion tests were performed on deposits from solution 1Na, 1Al and 1HA (deposition time 1 and 5 h). Results were compared with those obtained for deposits using solution 6.

Figure 11 shows potential/current curves in semi-logarithmic graphs (Tafel plots). The potential range goes from −300 mV to +300 mV with respect to the rest potential *Er*. All the coatings demonstrate very similar behaviour characterised by: (i) a current minimum at −450 mV, this may suggest the presence of a passivation phenomenon; the minimum current value (passivation current) is indicated by j_p; (ii) a current maximum ranging from −600 to −650 mV due to the activation of the oxidation (corrosion) process on the metal surface; the maximum current value (activation current) is indicated by j_a.

All the coatings show extremely low values of j_p and j_a (Table 7), meaning that they provide a good degree of protection.

For the 1-h electrodepositions, best results were achieved with solutions containing Na_2SO_4 or $Al_2(SO_4)_3$

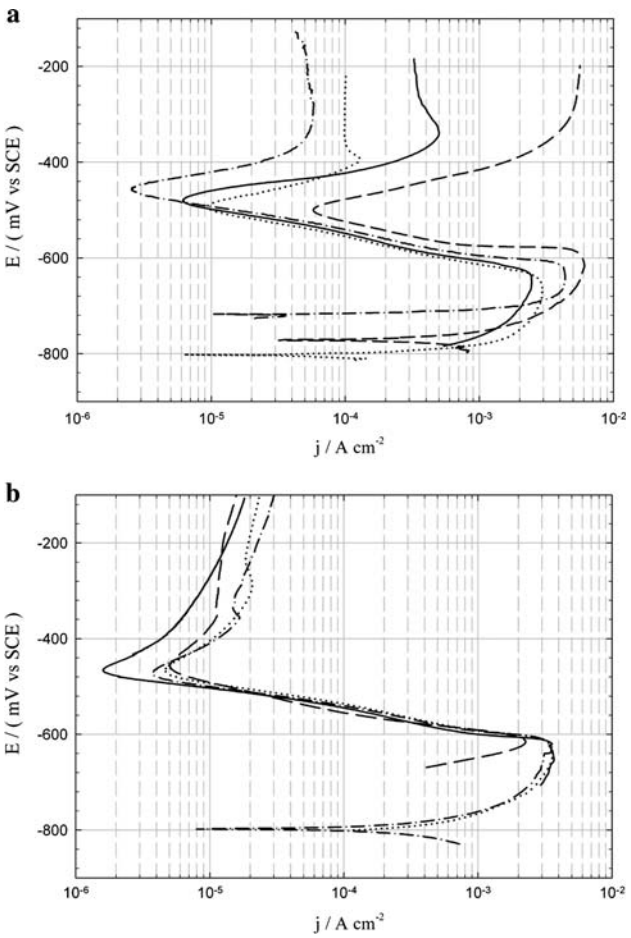

Fig. 11 Corrosion test (Tafel plot) on coating obtained with 1 h (**a**) and 5 h (**b**) electrodeposition with different bath compositions: solution 6 (solid line), solution 1HA (dashed line), solution 1Na (dotted-dashed line) and solution 1Al (dotted line)

Table 7 Values of j_p (passivation current) and j_a (activation current) for coatings obtained with different solutions and deposition times

Solution	1Na		1Al		1HA		6 (Fink)	
Deposition time	1 h	5 h	1 h	5 h	1 h	5 h	1 h	5 h
j_p (A cm^{-2})	2.6×10^{-6}	3.8×10^{-6}	9.0×10^{-6}	4.7×10^{-6}	5.9×10^{-5}	3.8×10^{-6}	6.0×10^{-6}	0.8×10^{-6}
j_a (A cm^{-2})	4.3×10^{-3}	3.5×10^{-3}	3.0×10^{-3}	3.5×10^{-3}	6.0×10^{-3}	2.3×10^{-3}	2.5×10^{-3}	3.5×10^{-3}

rather than H_2SO_4. This is confirmed by the pictures of Fig. 12a, b, c and d. The pictures were taken soon after the end of the corrosion test with a metallographic microscope. The corrosion attack begins beside the cracks of the coating, but the low j_a values suggest that the corrosion process does not reach the iron substrate. The coating from solution 1HA (Fig. 12c) presents much wider cracks responsible for more intense corrosion. The 5-h deposits show almost identical values of j_a and j_p at all concentrations. This confirms the excellent protection provided by the high thickness coatings obtained from alternative deposition baths.

4 Conclusions

An electrodeposition bath, alternative to those now in use, is proposed. Its main characteristics are: (i) low chromium trioxide content (100 g dm^{-3} instead of typical 250 or 400 g dm^{-3} values) (ii) ability to yield coatings with properties in line with those of the traditional coatings; (iii) the same current efficiency of the concentrated baths. Although the proposed new composition does not completely solve the problems related to the use of Cr(VI) compounds, it does make it possible to operate with a weaker deposition bath.

The only drawback is the decrease in the solution conductivity, which can be overcome by an increase in deposition time. Efforts to eliminate this problem using additives did not prove successful. However, they did allow the identification of two chemical species, Na_2SO_4 and $Al_2(SO_4)_3$, which can replace the sulphuric acid to produce shinier and smoother deposits.

A deposition bath was formulated able to give coatings with better properties than those obtained from conventional baths, especially as regards mean roughness, and, at the same time, the content of hexavalent chromium is significantly reduced.

The main future developments could be: (i) transfer of the results obtained on laboratory scale to industrial baths, working with larger samples in a pilot plant; (ii) developing an alternative method to increase the ionic strength of the solution, so that the problems connected to the longer deposition time and the lower throwing power can be solved.

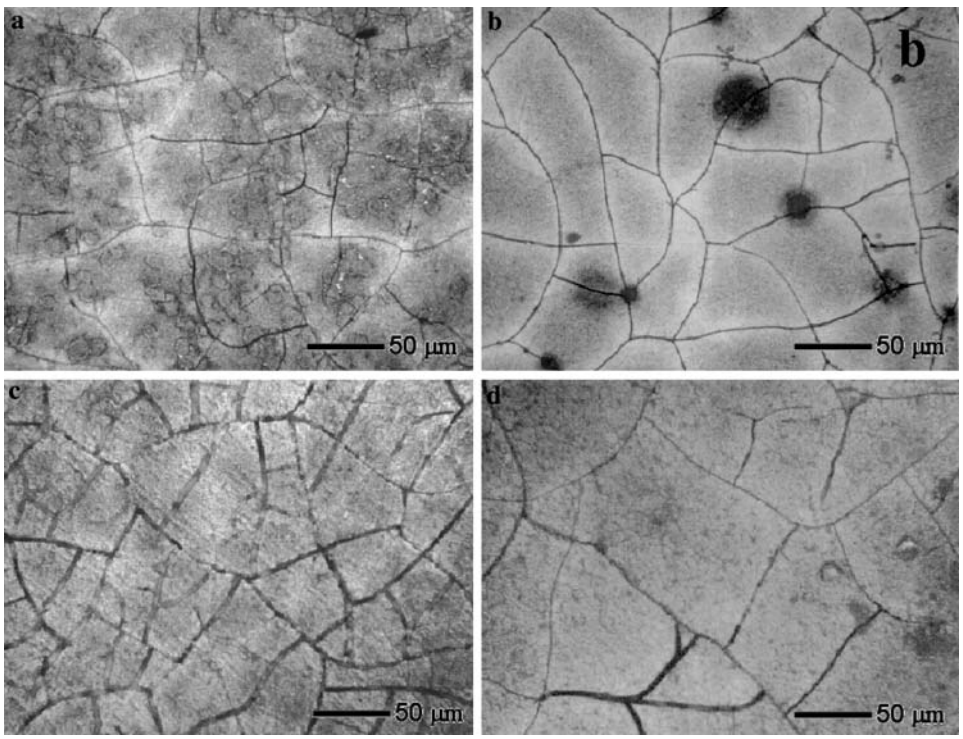

Fig. 12 Images of samples after corrosion tests; coatings obtained with electrodeposition of 1 h in different solutions: solution 1Na (**a**), 1Al (**b**), 1HA (**c**) and solution 6 (**d**)

References

1. Mandich NV (1998) Plat Surf Finish 85(12):91
2. Saiddington J, Hoey GR (1973) J Electrochem Soc 120:1475
3. Saiddington J, Hoey GR (1970) J Electrochem Soc 117:1012
4. Surviliene S, Jasulaitiene V, Nivinskiene O et al (2007) Appl Surf Sci 253:6738
5. Surviliene S, Bellozor S, Kurtinaitiene M et al (2004) Surf Coat Technol 176:193
6. Kok YN, Hovsepian PE (2006) Surf Coat Technol 201:3596
7. Zhixiang Z, Liping W, Li C et al (2006) Surf Coat Technol 201(6):2282
8. Petukhov IV, Shcherban' MG, Kichigin VI et al (2006) Prot Met 42(4):378
9. Surviliene S, Orlovskaja L, Biallozor S (1999) Surf Coat Technol 122:235
10. Muller E (1935) Trans Faraday Soc 31:1194
11. Muller E, Ekwall P (1929) Z Elektrochem 35:84
12. Muller E, Stscherbakow J (1929) Z Elektrochem 35:222
13. Muller E (1944) Z Elektrochem 50:172
14. Fink CG (1926) U.S. Pat. 1581188
15. Manahan SE (1994) Biotechnol Prog 11:235
16. Gupta VK, Shrivastawa AK, Jain N (2001) Water Res 35:4079
17. Pletcher D (1982) Industrial electrochemistry. Chapman and Hall Ltd., New York
18. http://www.csm-instruments.com/new/contenus/e/doc/bulletins/AB_18.pdf
19. Bard AJ, Faulkner LR (2001) Electrochemical methods. Fundamentals and applications, 2nd edn. Wiley, New York